Supporting Information

Intrinsic and/or Photo-Induced Antibacterial Activity of Bio-Based Dye-Functionalized Emulsion Templated Porous Polymers

Hassan Hayek[a], Pascal Boucq[b], Samir abbad Andaloussi[c], Sebastijan Kovačič[d,e], Antoine Debuigne[b]*, Davy-Louis Versace[a*]

[a] University Paris-Est Creteil, CNRS, ICMPE, UMR 7182, 94320 Thiais, France

[b] Center for Education and Research on Macromolecules (CERM), CESAM Research Unit, Chemistry Department, University of Liège (ULiege), Quartier Agora, 13 Allée du Six Août, Sart-Tilman, B-4000 Liège, Belgium.

[c] Université Paris-Est Créteil (UPEC), Laboratoire Eau, Environnement, Systèmes Urbains (LEESU), UMR-MA 102, 61 avenue Général de Gaulle, 94010 Créteil Cedex, France

[d] Catalysis and Organic Synthesis research group, Laboratory for Organic and Polymer Chemistry, Faculty of Chemistry and Chemical Engineering, University of Maribor, Smetanova 17, SI-2000 Maribor, Slovenia.

[e] National Institute of Chemistry, Hajdrihova 19, SI-1001 Ljubljana, Slovenia

*Corresponding authors: Antoine Debuigne adebuigne@uliege.be , Davy-Louis Versace davy-louis.versace@u-pec.fr

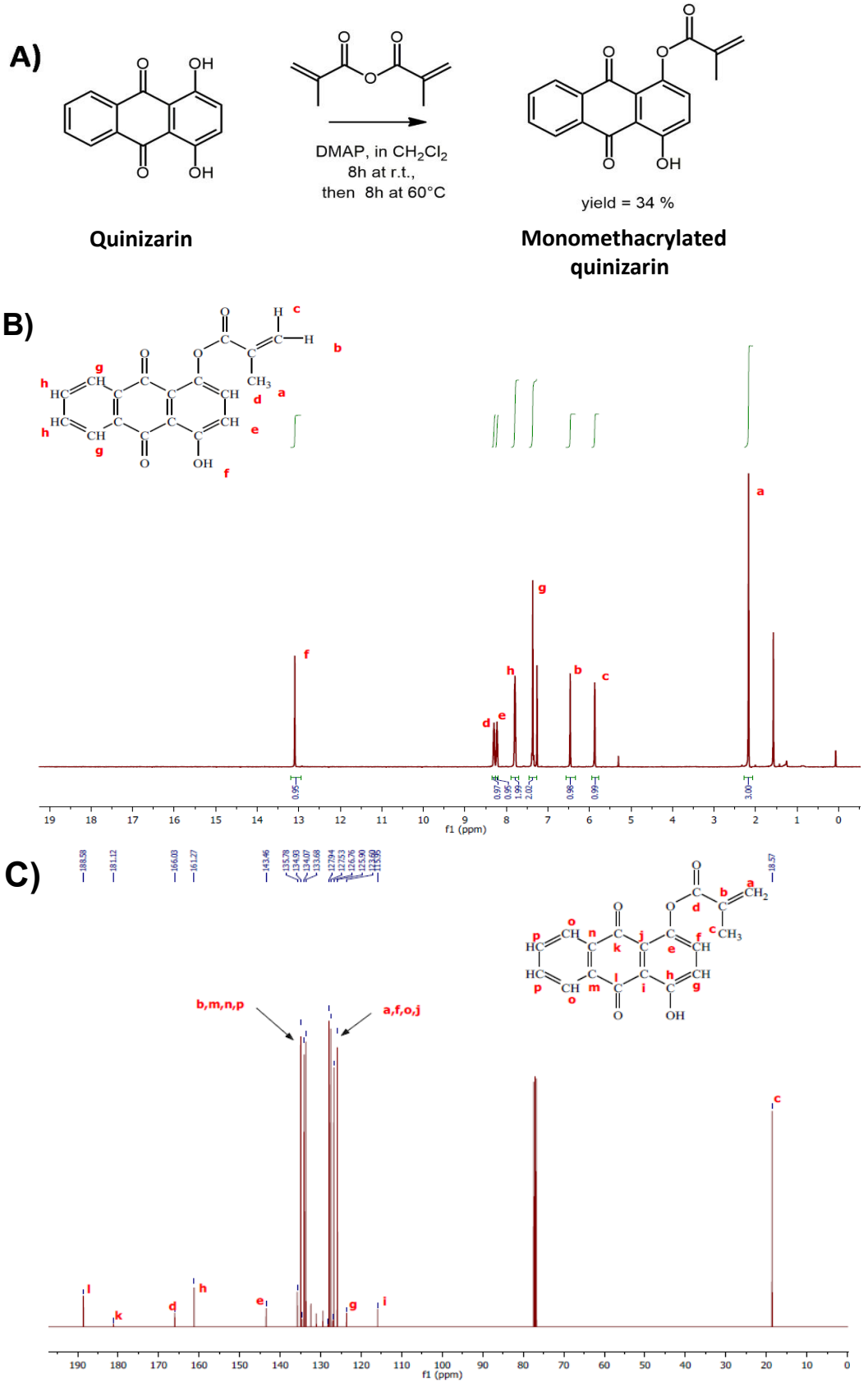

Figure S1. (A) General reaction synthesis and (B) ^{1}H NMR of the methacrylated quinizarin "Q" in $CDCl_3$ and (C) ^{13}C NMR of the methacrylated quinizarin "Q" in $CDCl_3$.

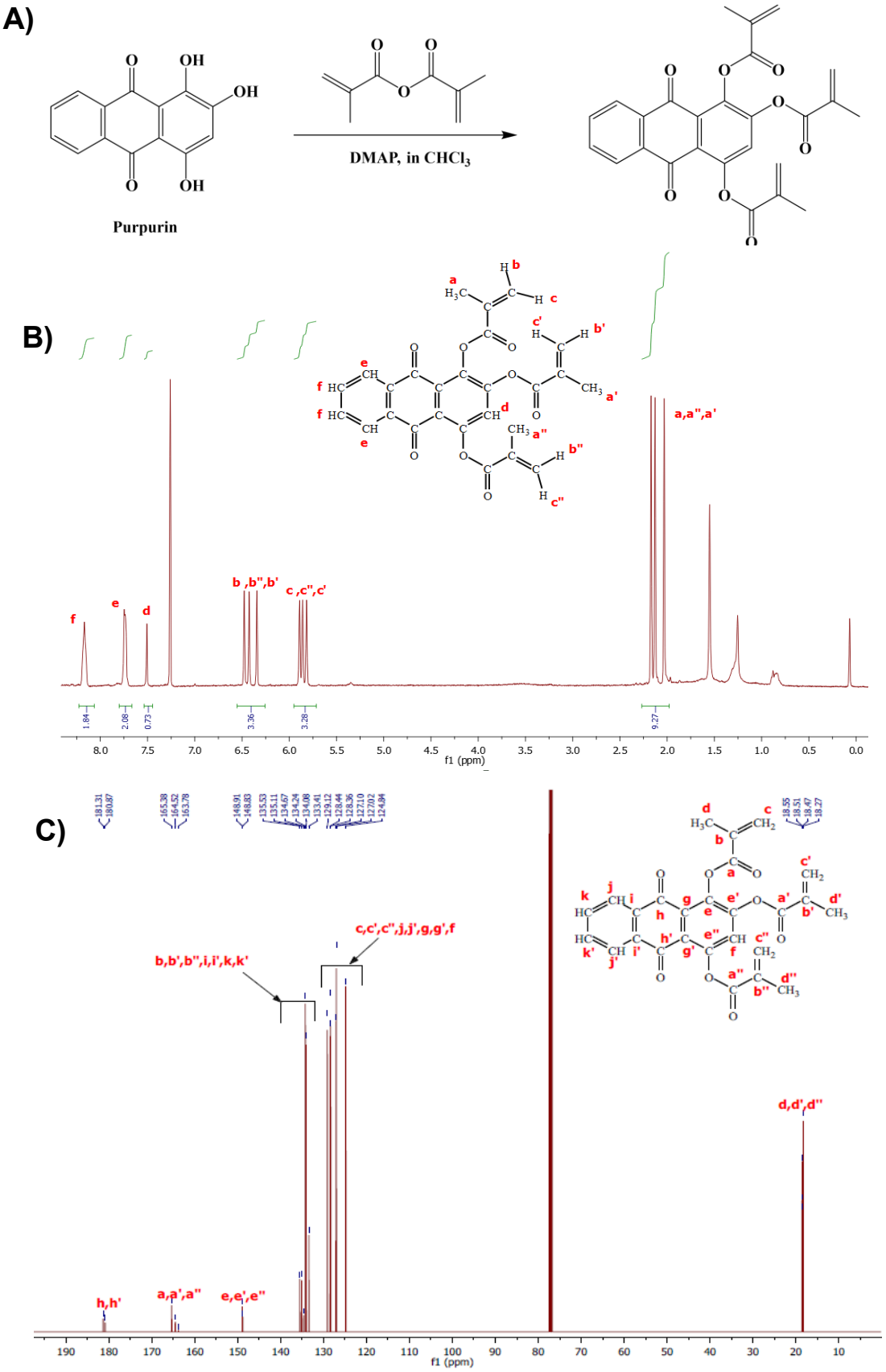

Figure S2. (A) General reaction synthesis and (B) ^{1}H NMR of the methacrylated purpurin "P" in $CDCl_3$ and (C) ^{13}C NMR of the methacrylated purpurin "P" in $CDCl_3$.

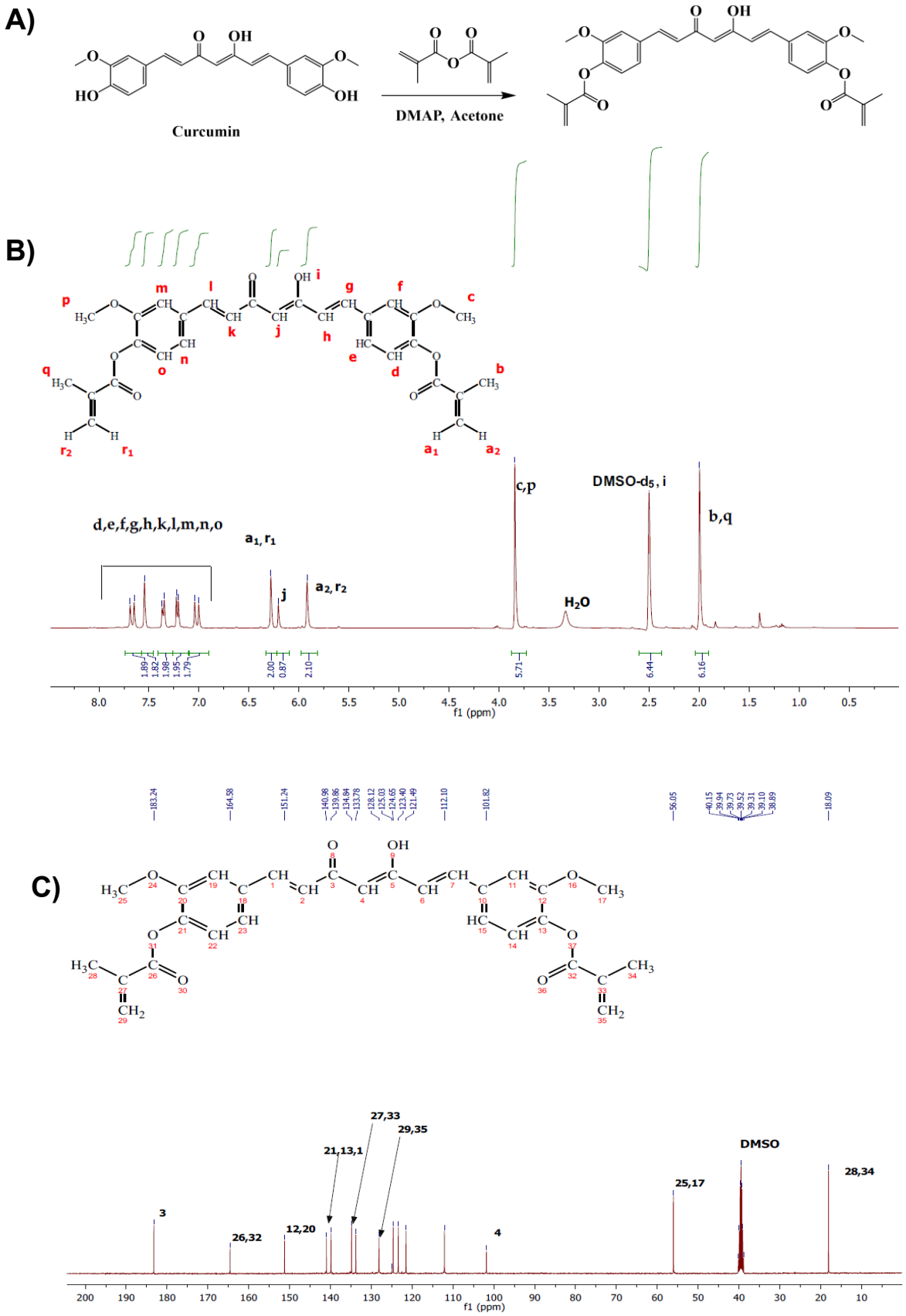

Figure S3. (A) General reaction synthesis, (B) ^{1}H NMR of the methacrylated curcumin "C" in DMSO and (C) ^{13}C NMR of the methacrylated curcumin "C" in DMSO.

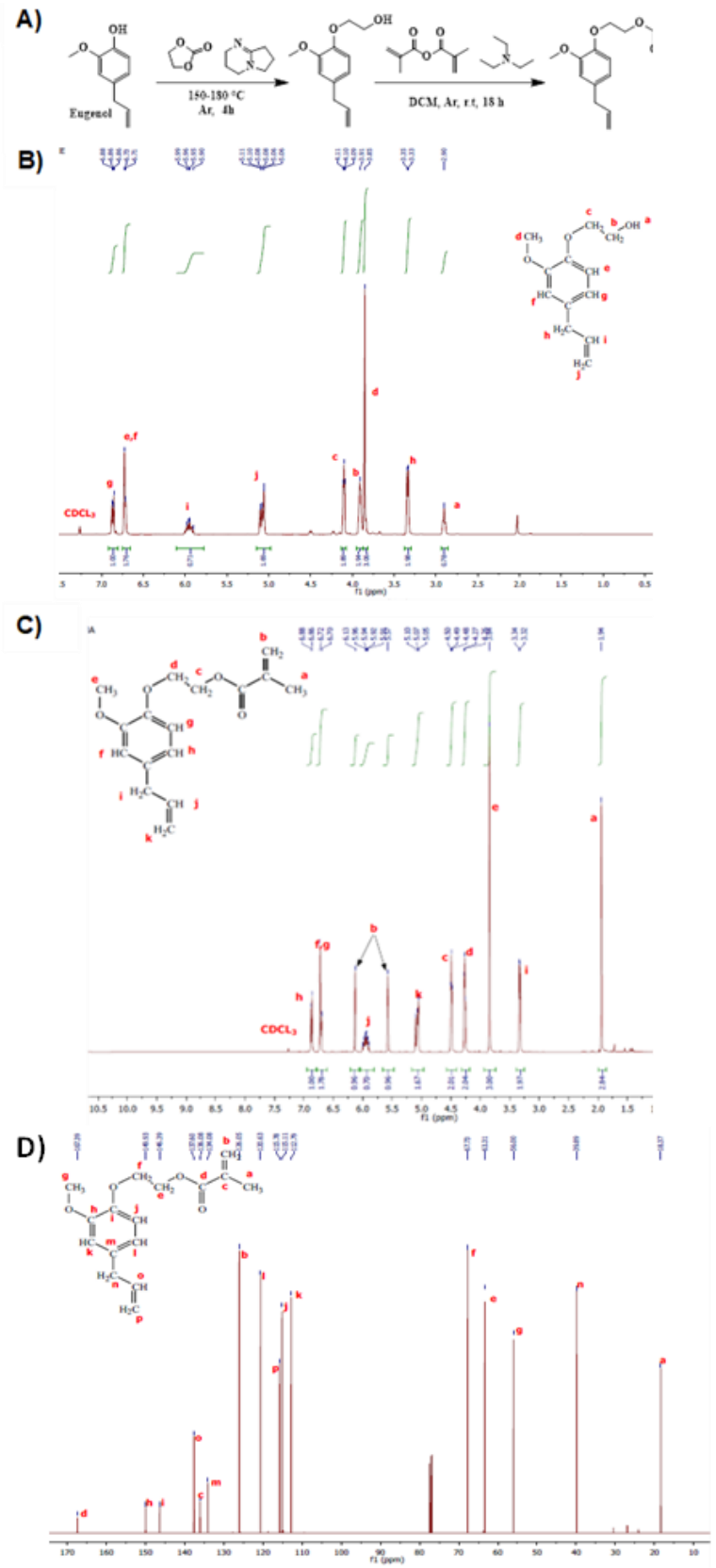

Figure S4. (A) General reaction synthesis, (B) ^{1}H NMR of hydroxylethyl derivative of eugenol and (C) ^{1}H NMR of the methacrylated eugenol "E" in $CDCl_3$ and (D) ^{13}C NMR of the methacrylated eugenol "E" in $CDCl_3$.

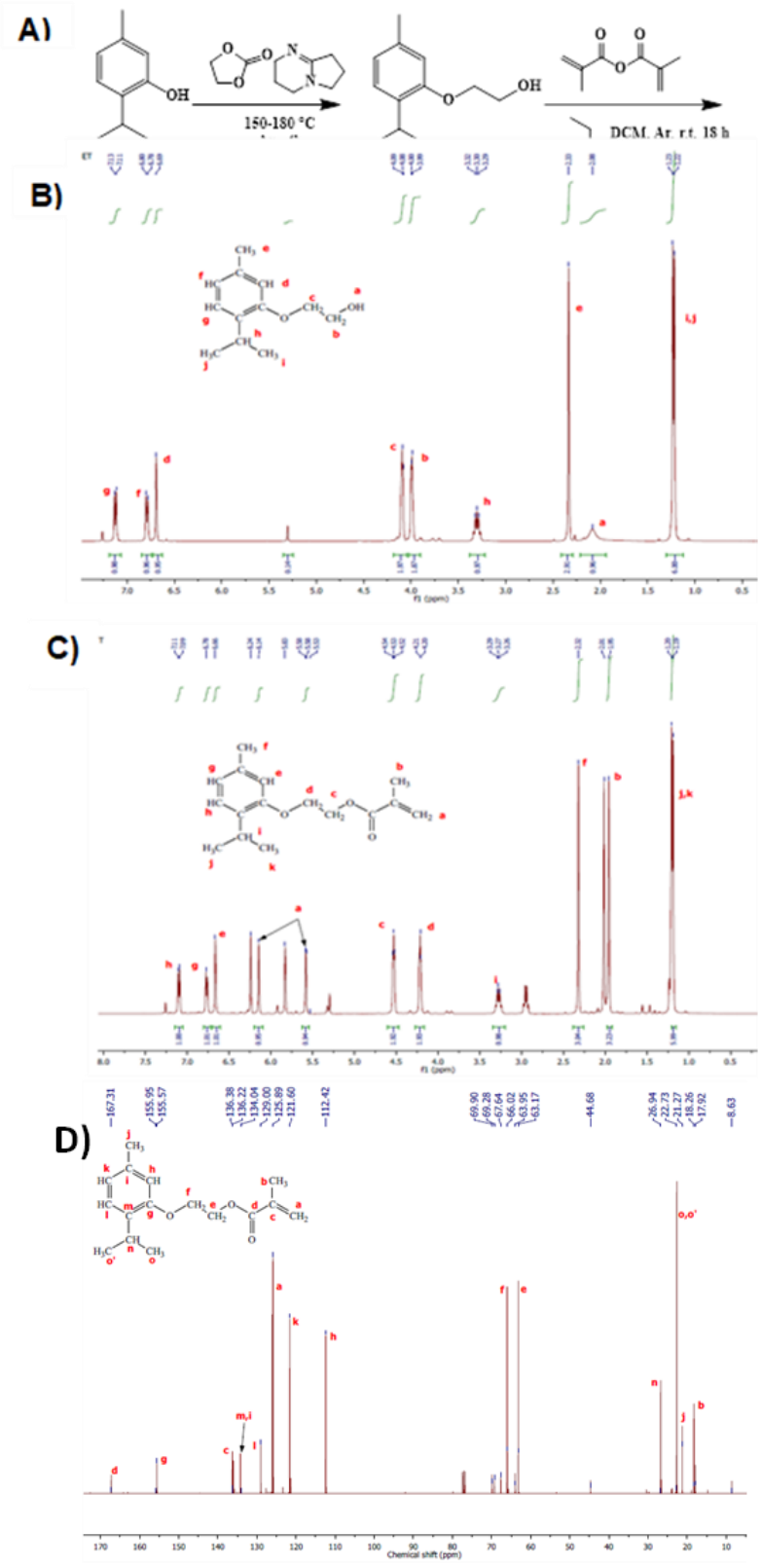

Figure S5. (A) General reaction **s**ynthesis, (B) ^{1}H NMR of the hydroxylethyl derivative of thymol, (C) ^{1}H NMR of the methacrylated thymol "T" in $CDCl_3$ and D) ^{13}C NMR of the methacrylated thymol "T" in $CDCl_3$.

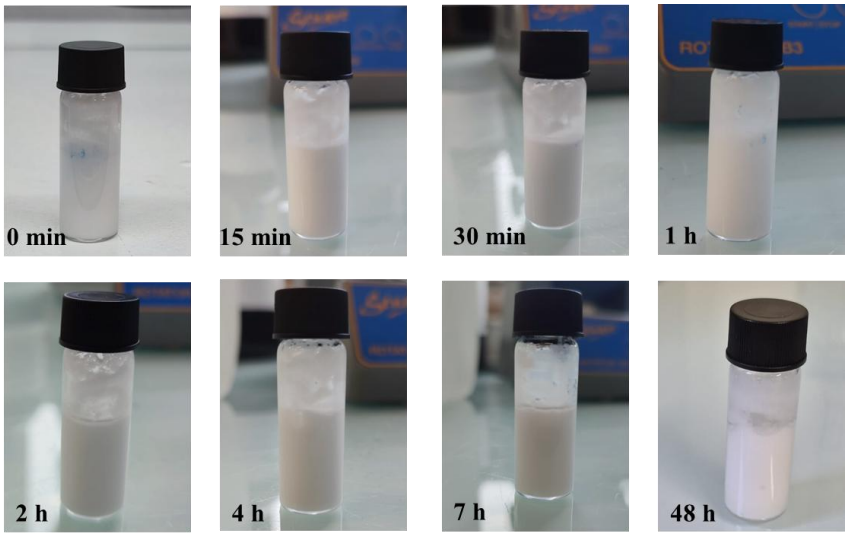

Figure S6. Pictures of the eugenol-based HIPE (formulated without AIBN) at different time at 60 °C, proving the stability of the emulsion under the polymerization conditions.

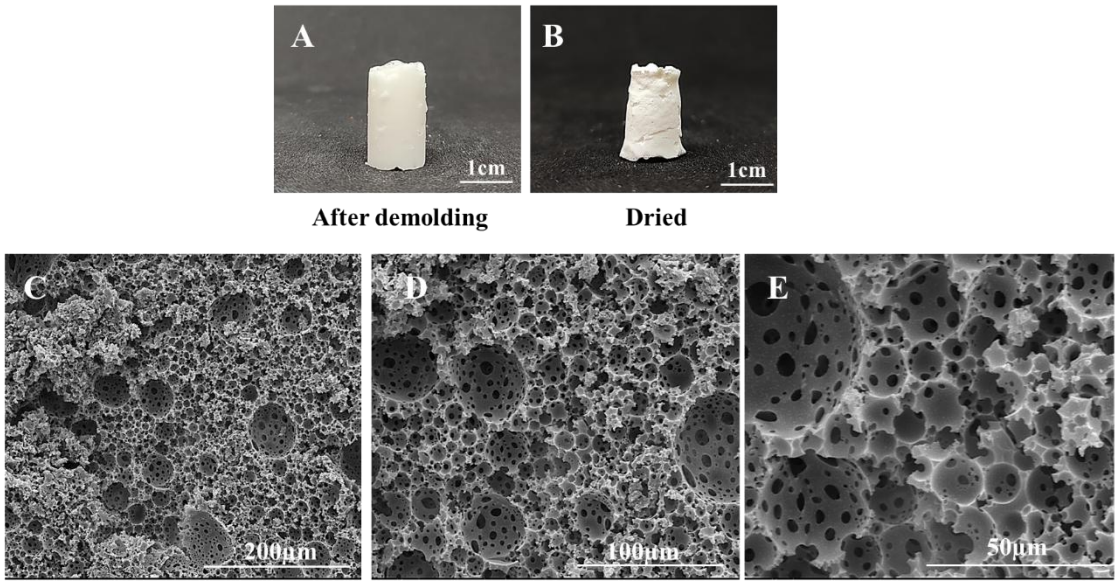

Figure S7. Pictures of the PHA: (A) after demolding (B) after drying, SEM images of the PolyHIPE showing its porous structure at different magnifications: (C) 500×, (D) 1000×, and (E) 2500×.

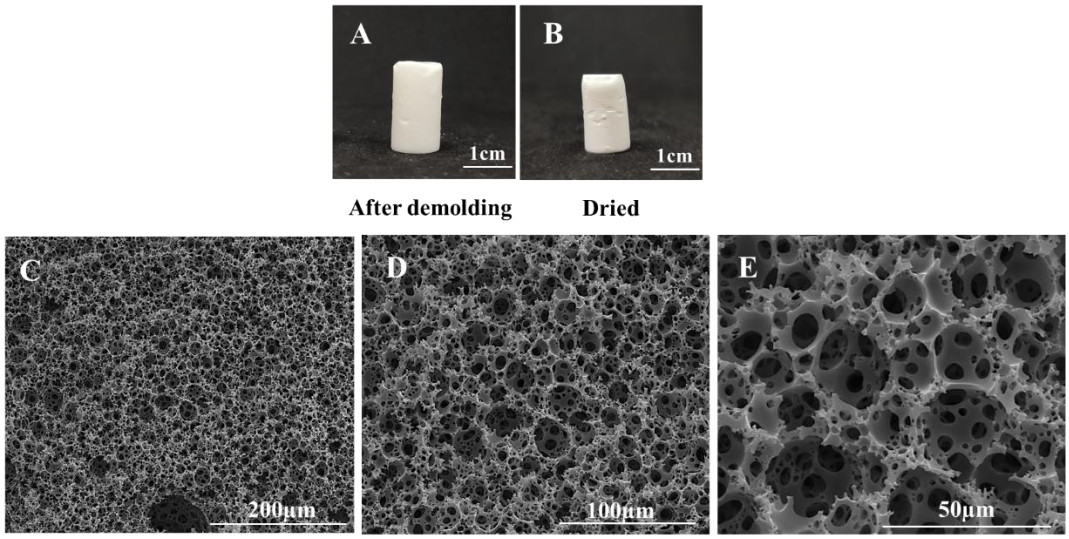

Figure S8. Pictures of the PHE: (A) after demolding (B) after drying, SEM images of the PolyHIPE showing its porous structure at different magnifications: (C) 500×, (D) 1000×, and (E) 2500×.

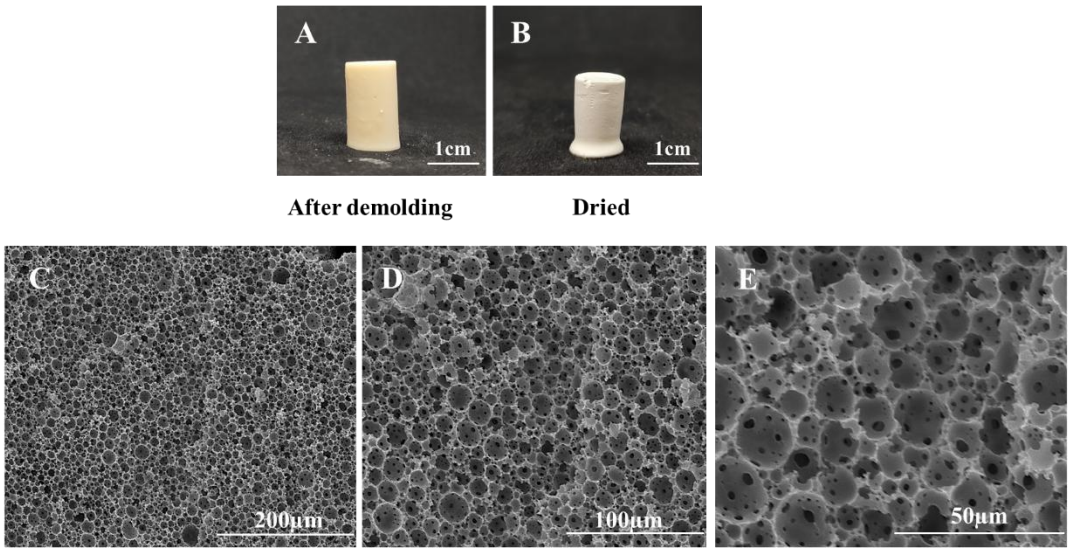

Figure S9. Pictures of the PHT: (A) after demolding (B) after drying, SEM images of the PolyHIPE showing its porous structure at different magnifications: (C) 500×, (D) 1000×, and (E) 2500×.

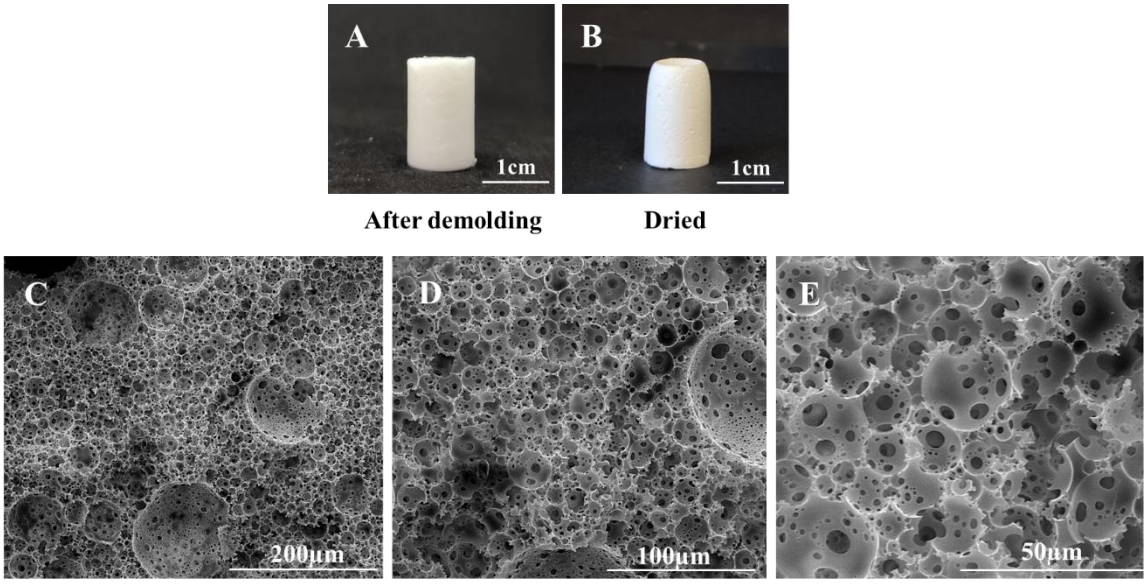

Figure S10. Pictures of the $PHA_{25}E_{75}$: (A) after demolding (B) after drying, SEM images of the PolyHIPE showing its porous structure at different magnifications: (C) 500×, (D) 1000×, and (E) 2500×.

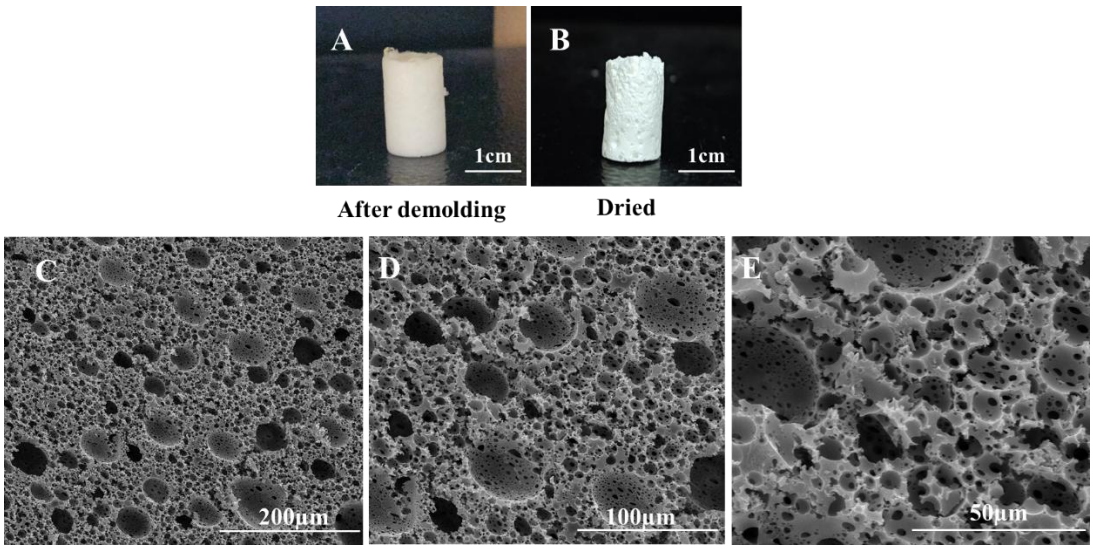

Figure S11. Pictures of the $PHA_{75}E_{25}$: (A) after demolding (B) after drying, SEM images of the PolyHIPE showing its porous structure at different magnifications: (C) 500×, (D) 1000×, and (E) 2500×.

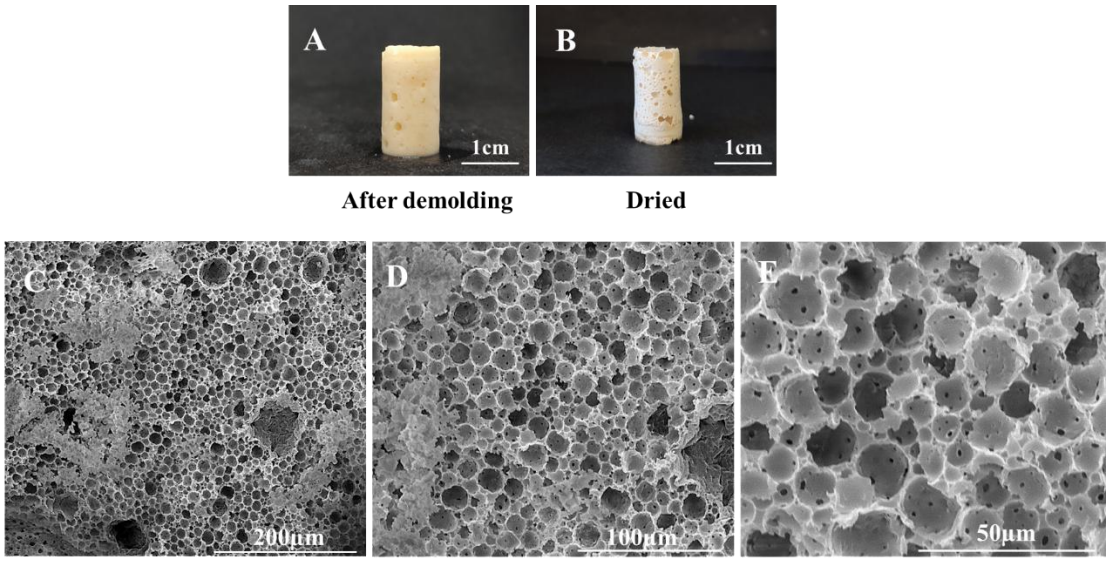

Figure S12. Pictures of the $PHA_{25}T_{75}$: (A) after demolding (B) after drying, SEM images of the PolyHIPE showing its porous structure at different magnifications: (C) 500×, (D) 1000×, and (E) 2500×.

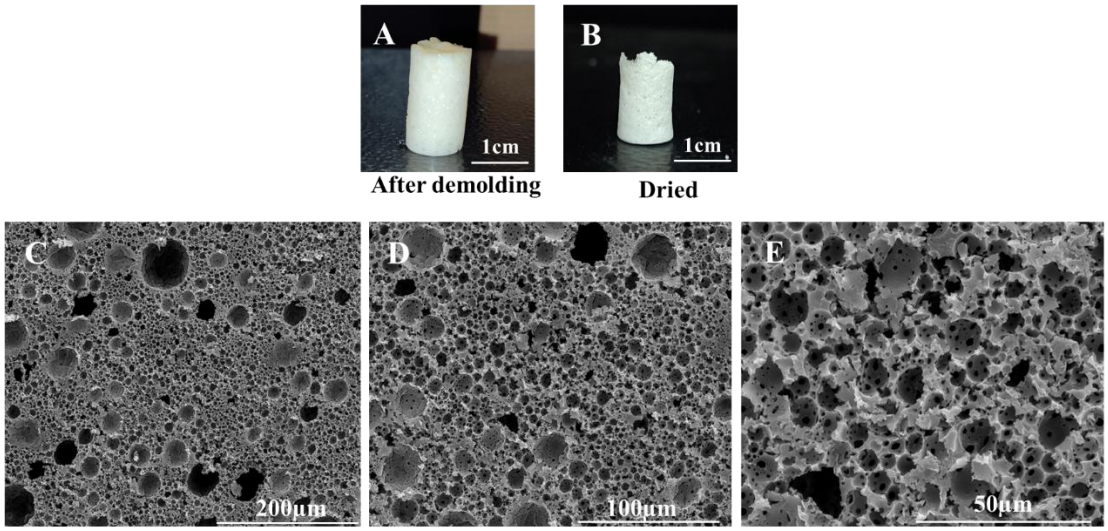

Figure S13. Pictures of the $PHA_{75}T_{25}$: (A) after demolding (B) after drying, SEM images of the PolyHIPE showing its porous structure at different magnifications: (C) 500×, (D) 1000×, and (E) 2500×.

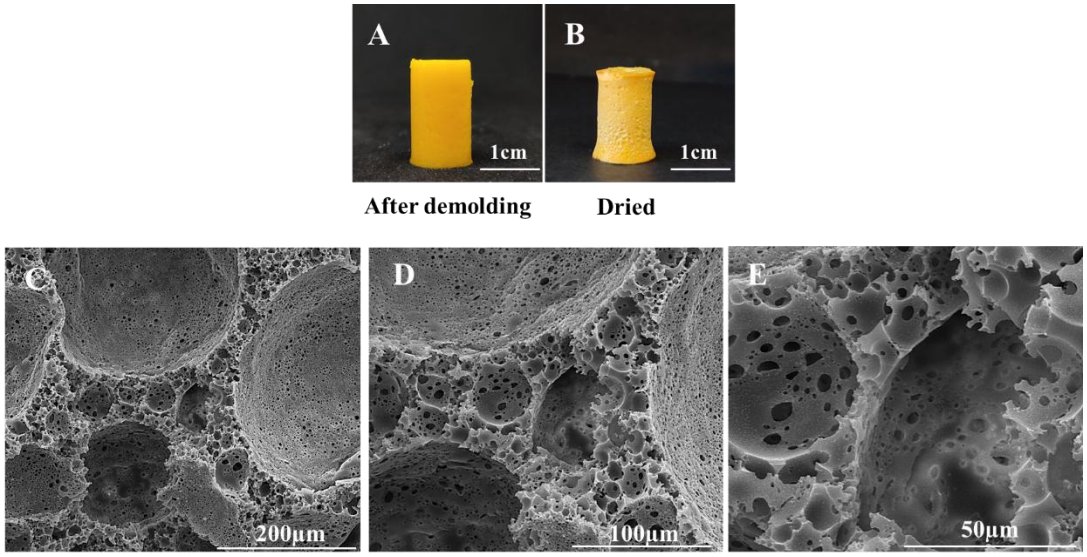

Figure S14. Pictures of the PHAQ: (A) after demolding (B) after drying, SEM images of the PolyHIPE showing its porous structure at different magnifications: (C) 500×, (D) 1000×, and (E) 2500×.

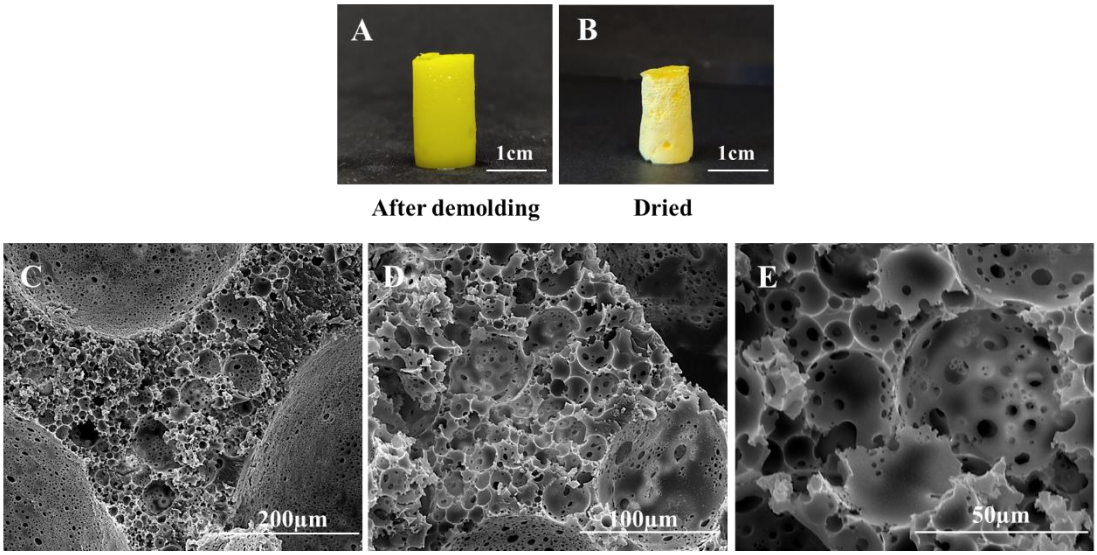

Figure S15. Pictures of the PHAC: (A) after demolding (B) after drying, SEM images of the PolyHIPE showing its porous structure at different magnifications: (C) 500×, (D) 1000×, and (E) 2500×.

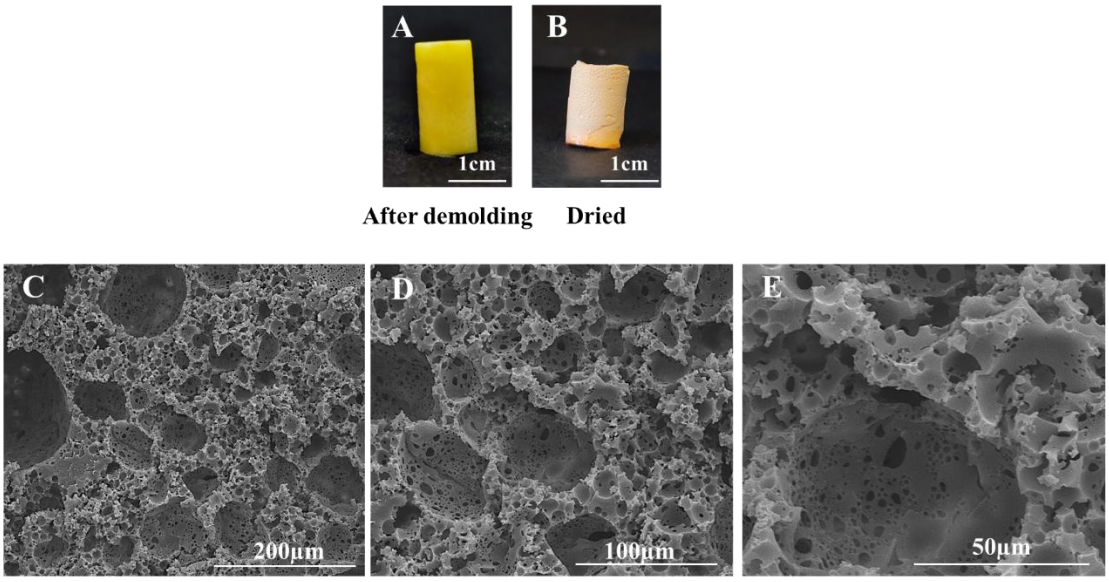

Figure S16. Pictures of the PHAP: (A) after demolding (B) after drying, SEM images of the PolyHIPE showing its porous structure at different magnifications: (C) 500×, (D) 1000×, and (E) 2500×.

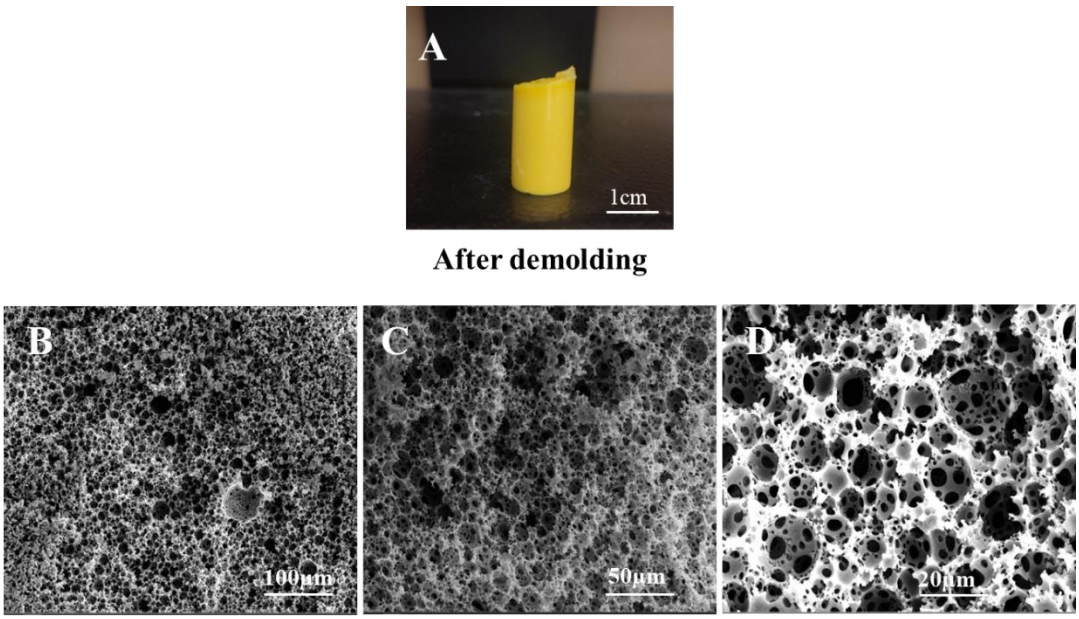

Figure S17. Picture of the PHEQ: (A) after demolding, SEM images of the PolyHIPE showing its porous structure at different magnifications: (B) 500×, (C) 1000×, and (D) 2500×.

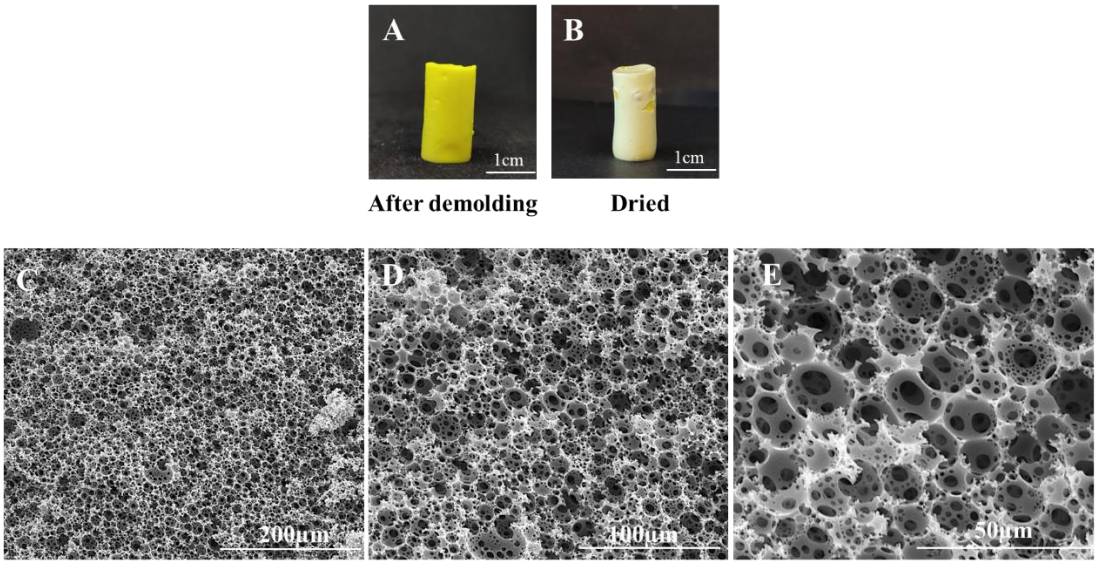

Figure S18. Pictures of the PHEC: (A) after demolding (B) after drying, SEM images of the PolyHIPE showing its porous structure at different magnifications: (C) 500×, (D) 1000×, and (E) 2500×.

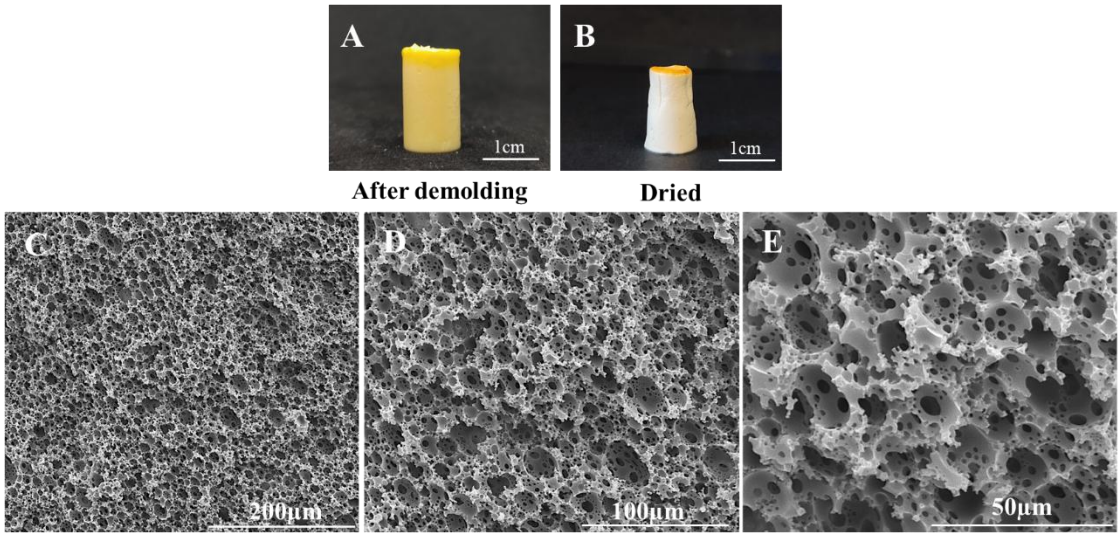

Figure S19. Pictures of the PHEP: (A) after demolding (B) after drying, SEM images of the PolyHIPE showing its porous structure at different magnifications: (C) 500×, (D) 1000×, and (E) 2500×.

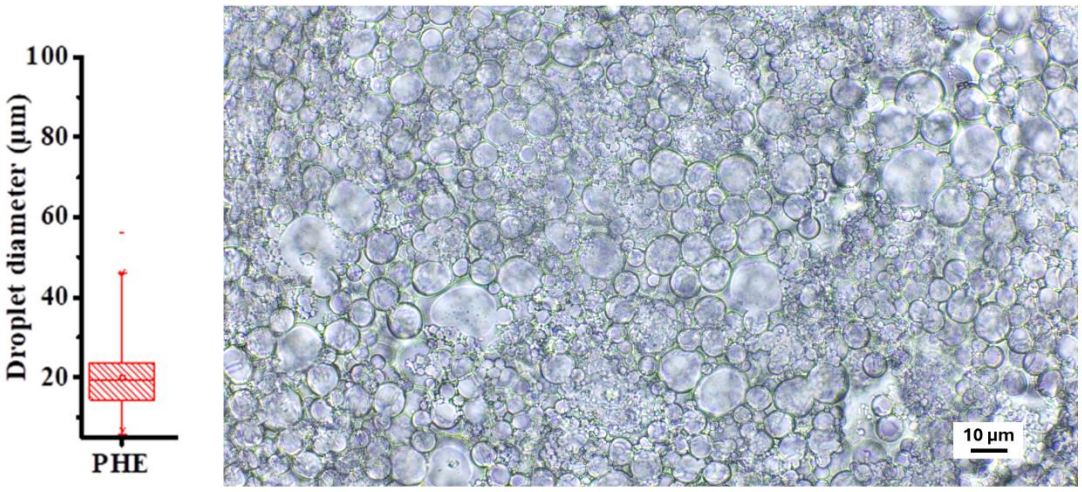

Figure S20. Optical microscopy image and box-and-whisker plot of droplet diameter of an eugenol-based HIPE (formulation used for the preparation of PHE).

Table S1. Densities, porosities and specific surface area of polyHIPEs.

Samples	PHA	PHAC	PHAP	PHAQ	PHE	PHT
ρ_{PH} [g·cm^{-3}][a]	0.18	0.12	0.14	0.18	0.13	0.19
ρ_{P} [g·cm^{-3}][b]	1.5922	1.2822	1.4367	1.2804	1.5442	1.2225
P [%][c]	88	91	90	86	92	84
S_{BET} [m^2·g^{-1}][d]	1.4	0.5	3.1	4.6	2.6	4.3

[a] Dry polyHIPE density; [b] skeletal polymer density determined by He-pycnometry; [c] porosity and [d] specific surface area.

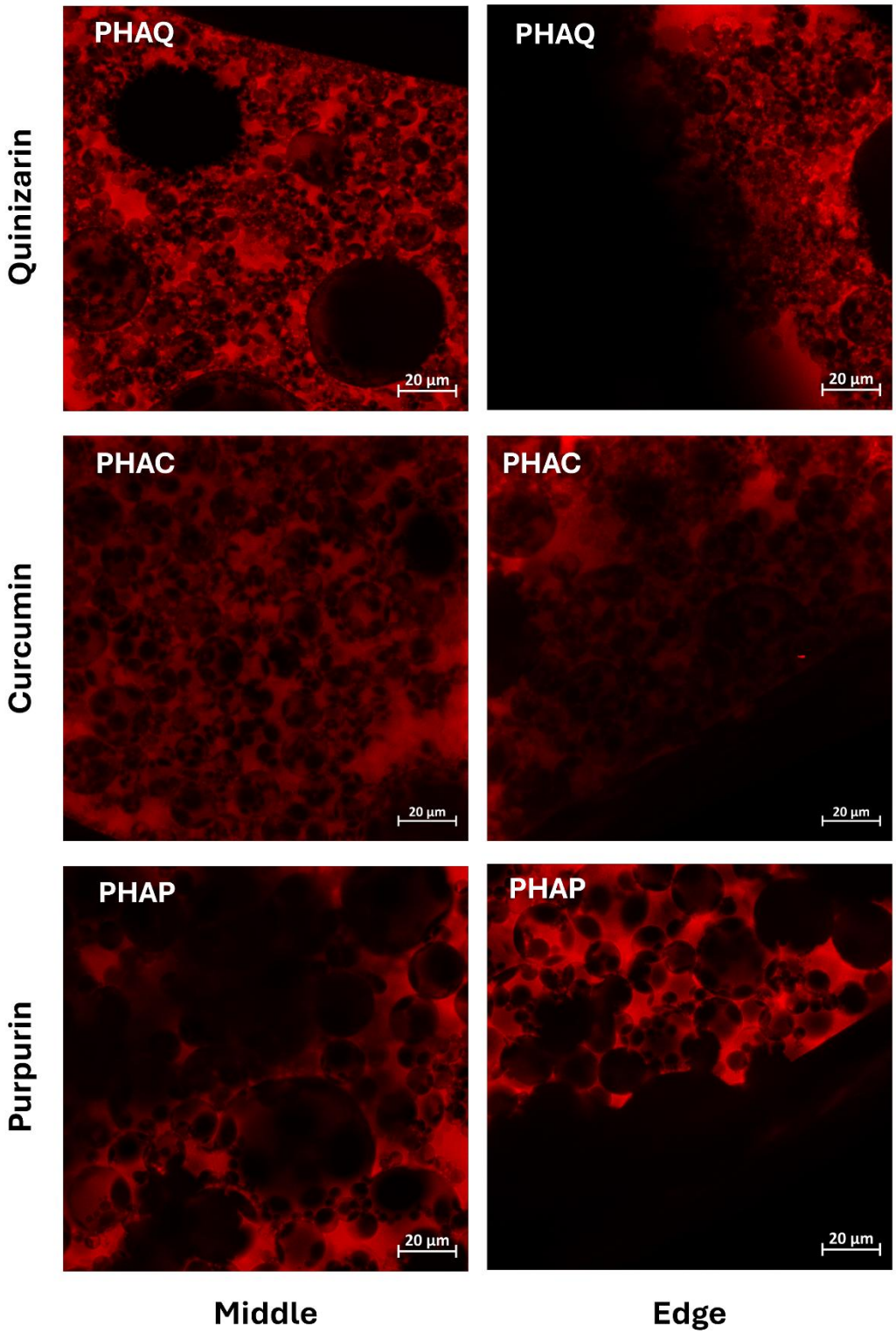

Figure S21. Confocal microscopy analyses at the center and at the edges of AESO-based polyHIPEs functionalized by quinizarine, curcumin and purpurin (PHAQ, PHAC, PHAP, respectively). A 405 nm laser was used for samples containing curcumin (excitation 420-450 nm and emission 500-550 nm) whereas a 488 nm laser was used for the sample functionalized with purpurin (excitation 450-500 nm and emission 550-600 nm) and quinizarin (excitation 450-500 nm and emission 550-650 nm).

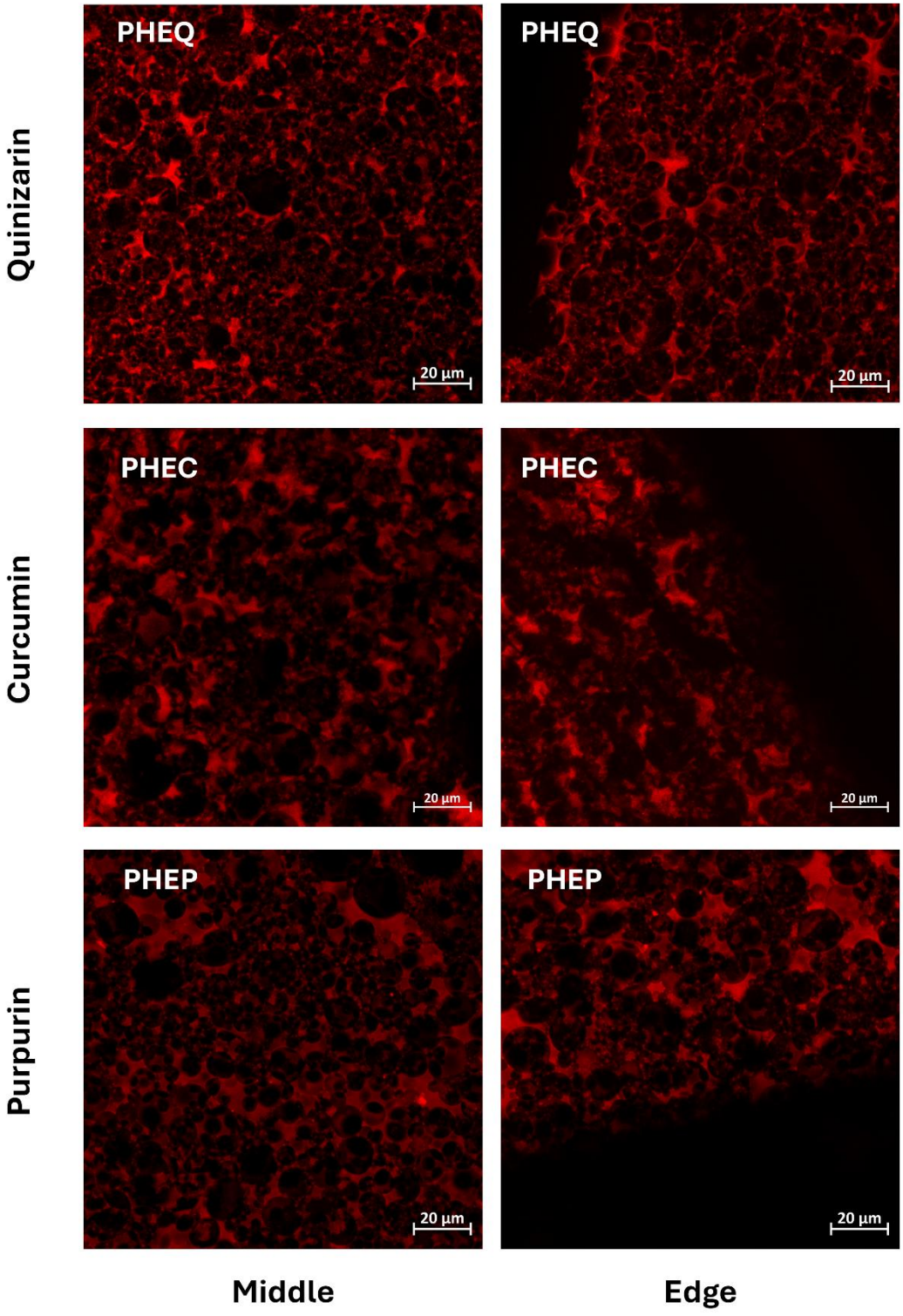

Figure S22. Confocal microscopy analyses at the center and at the edges of eugenol-based polyHIPEs functionalized by quinizarine, curcumin and purpurin (PHEQ, PHEC, PHEP, respectively). A 405 nm laser was used for samples containing curcumin (excitation 420-450 nm and emission 500-550 nm) whereas a 488 nm laser was used for the sample functionalized with purpurin (excitation 450-500 nm and emission 550-600 nm) and quinizarin (excitation 450-500 nm and emission 550-650 nm).

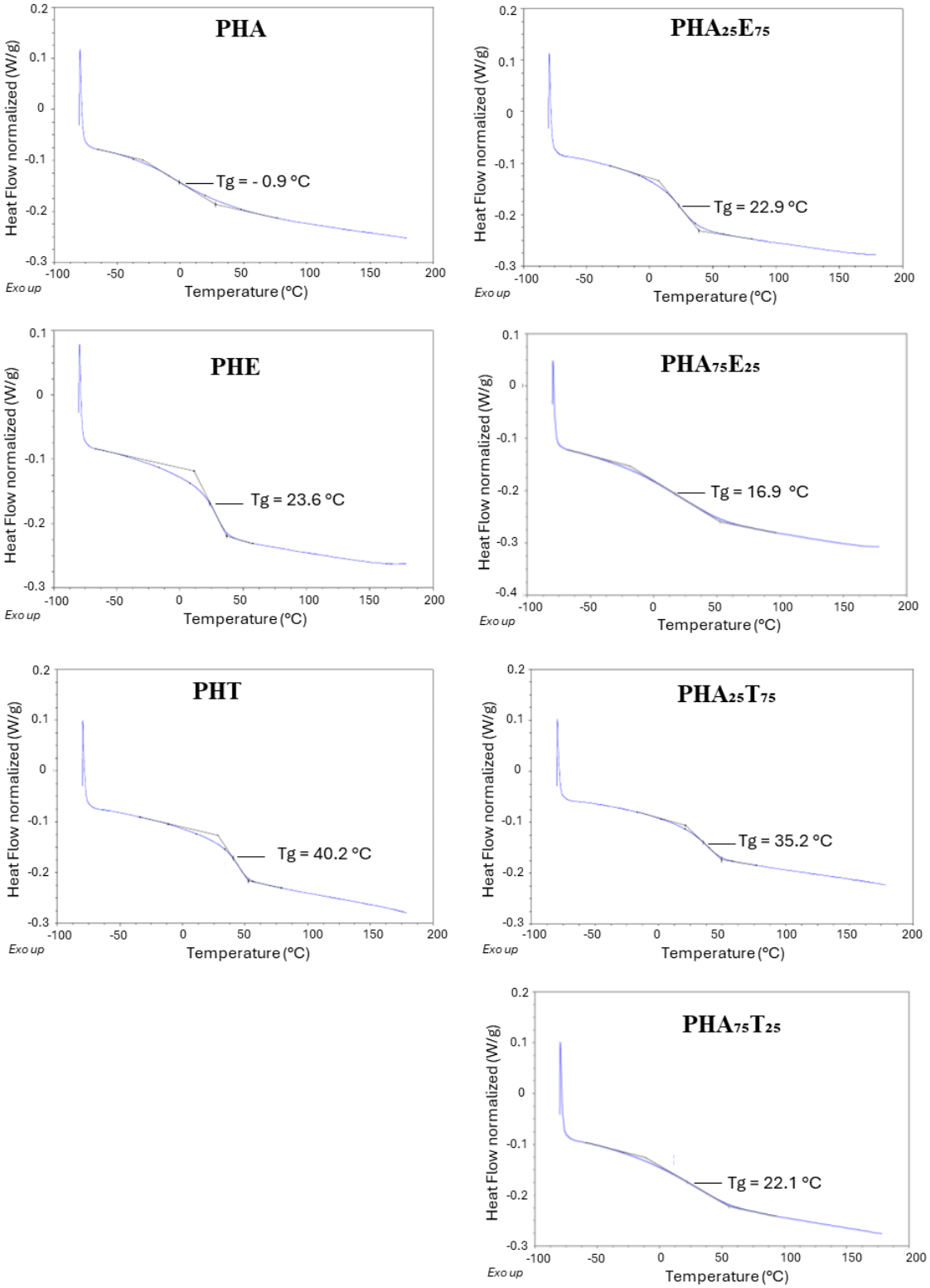

Figure S23. DSC curves of polyHIPEs formulated with different monomers (AESO, "T" and "E").

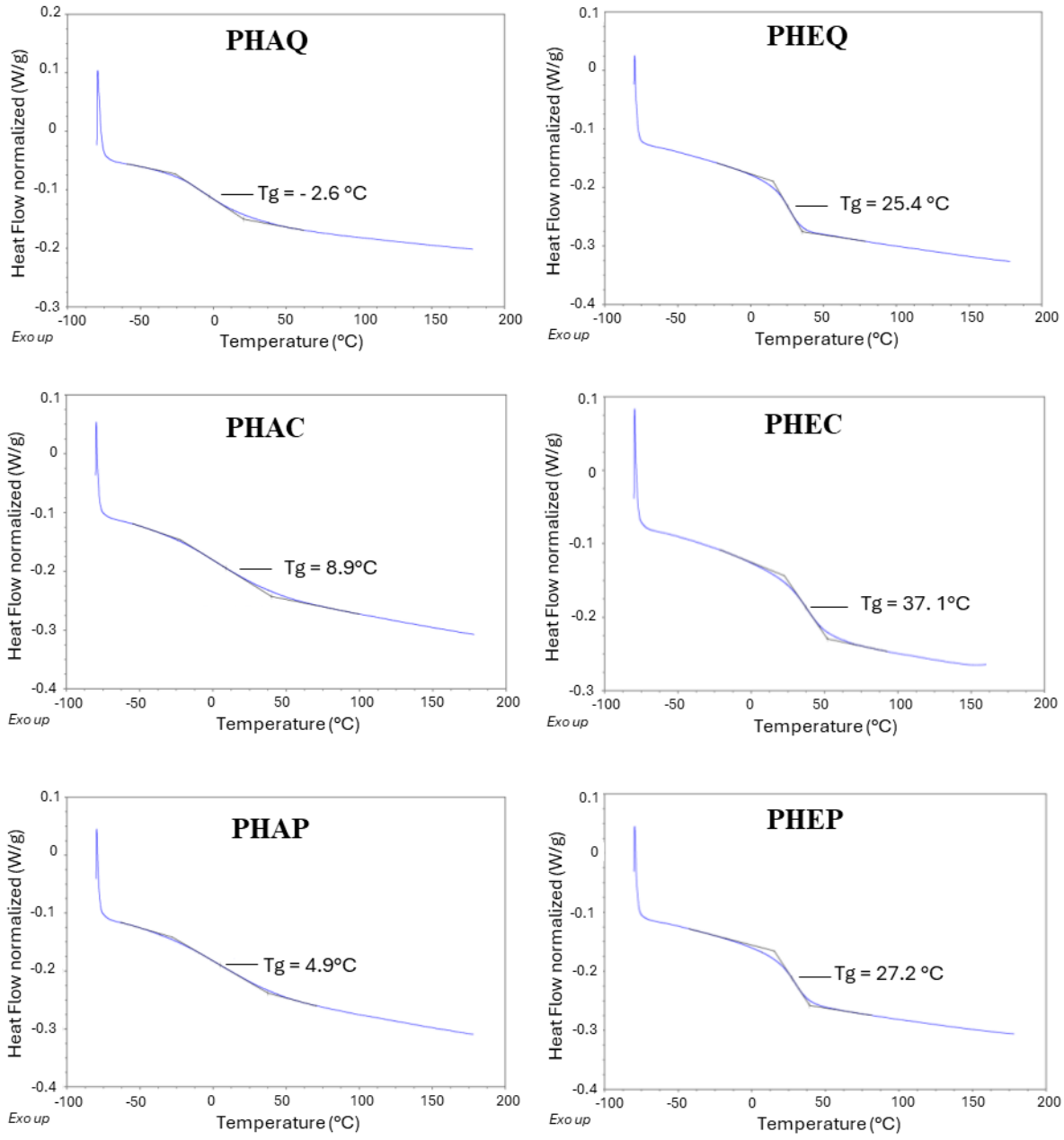

Figure S24. DSC curves of polyHIPEs incorporating dyes (quinizarin, purpurin and curcumin derivatives).

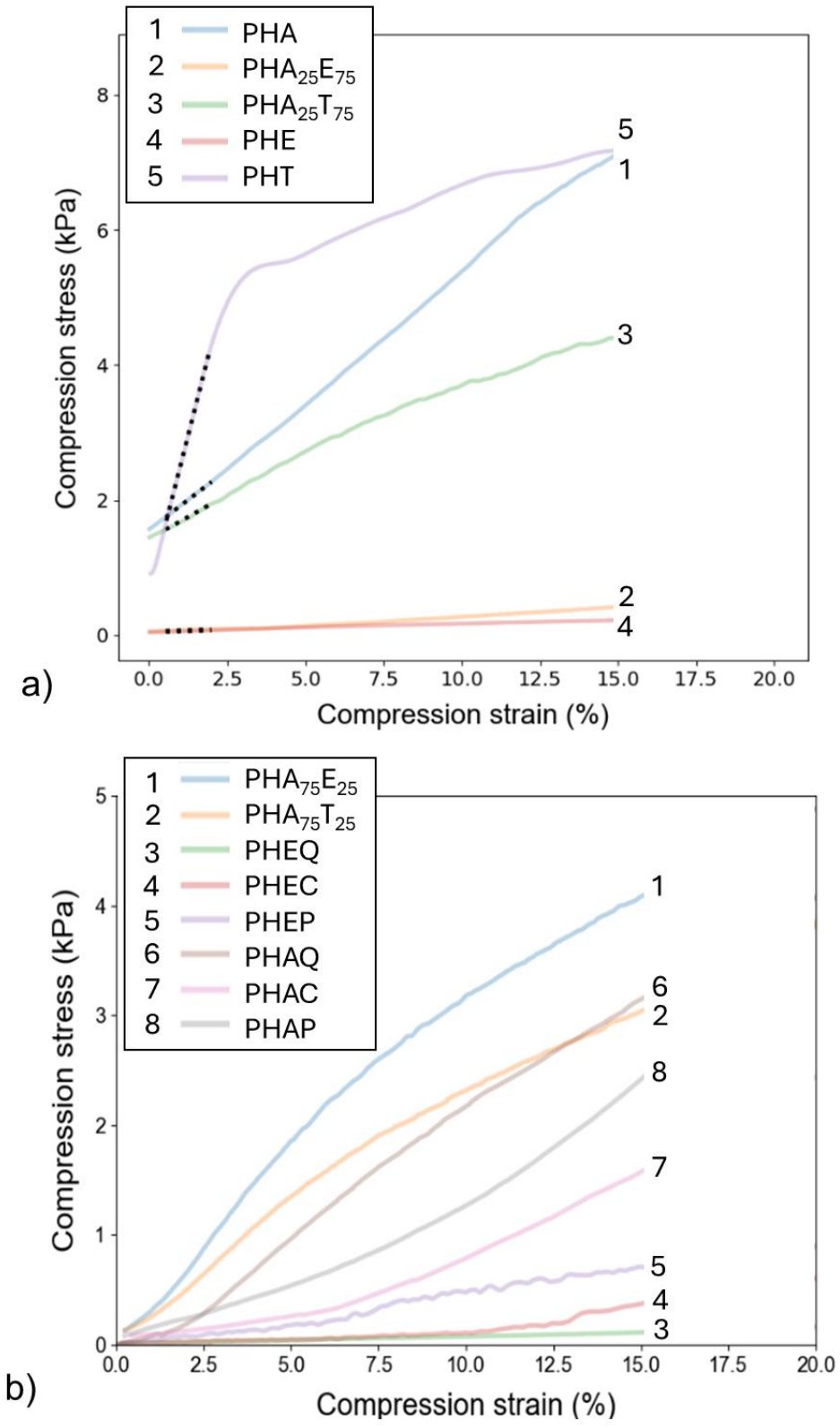

Figure S25. DMA curves of polyHIPEs with and without dyes.

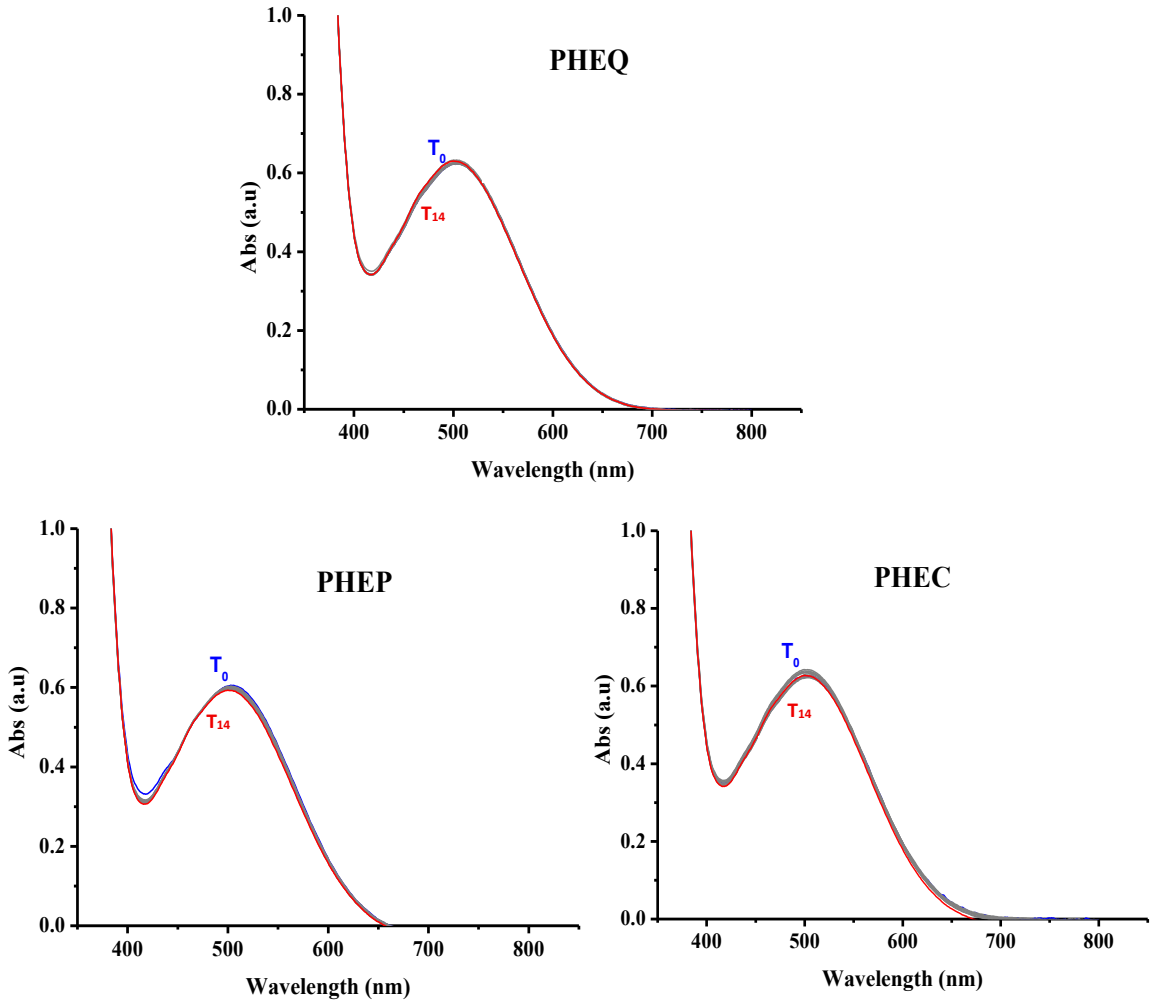

Figure S26. Evolution of the absorbance of TPCPD solution upon irradiation at 405 nm (100 mW.cm^{-2}) in the presence of polyHIPEs (PHEQ, PHEP or PHEC) T_0 = without irradiation, T_{14} = after 14 min of irradiation.

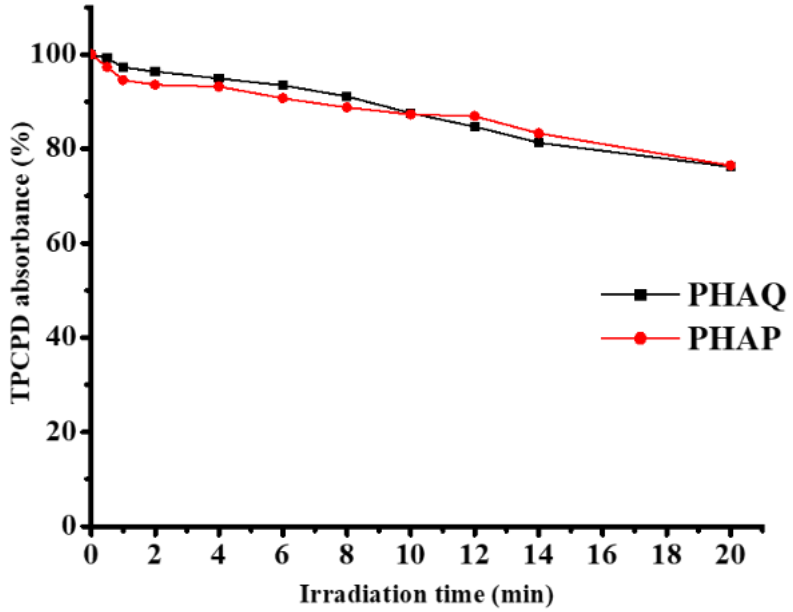

Figure S27. Plots of the TPCPD absorbance upon irradiation under solar-simulated light with an intensity of 240 μmol·m^{-2}·s^{-1} PPFD (Photosynthetic Photon Flux Density) in the presence of PHAQ or PHAP.

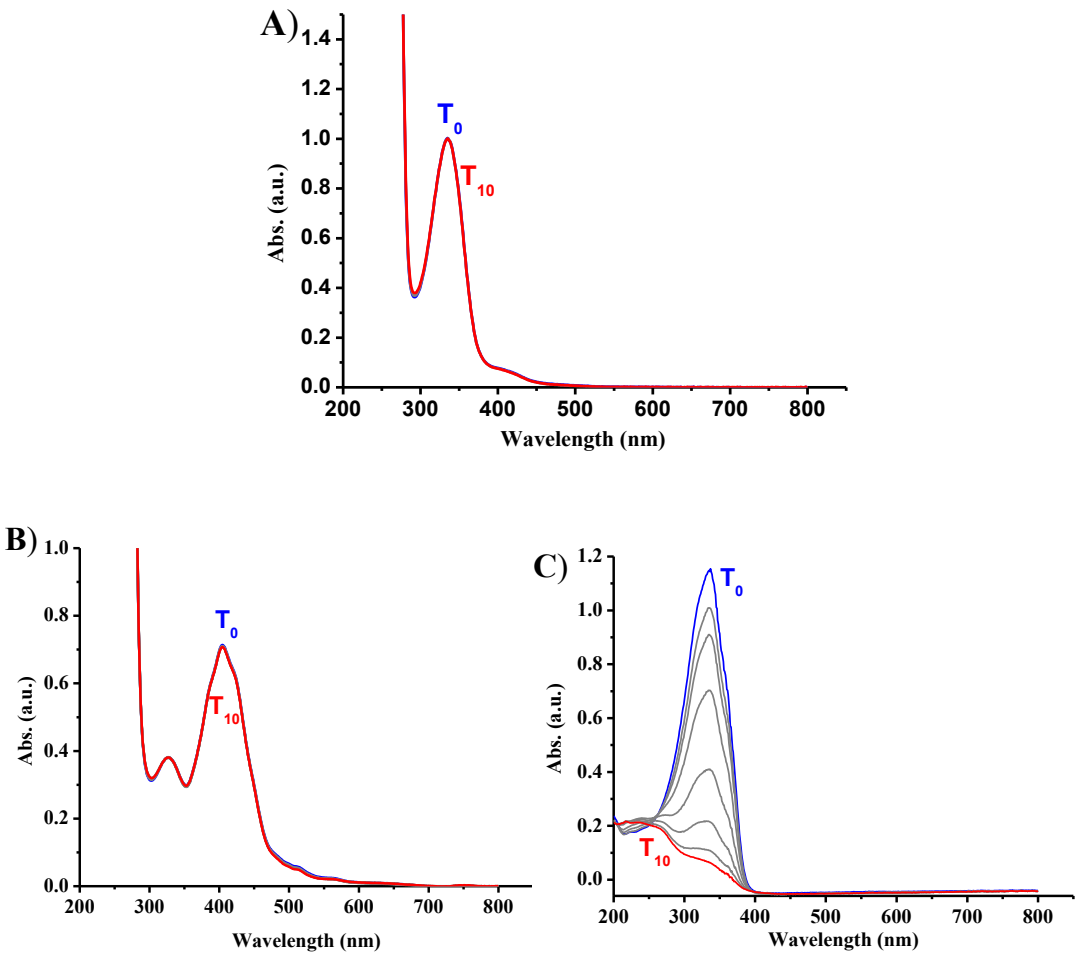

Figure S28. Photolysis of (A) methacrylated purpurin in ACN ([P] = 1.2×10^{-4} M), (B) methacrylated quinizarin in ACN ([Q] = 9.2×10^{-5}M), (C) methacrylated curcumin in ethanol ([C] = 1.98×10^{-5} M), upon irradiation at 405 nm (100 mW.cm^{-2}) for 10 min. T_0 = without irradiation, T_{10} = after 10 min of irradiation.

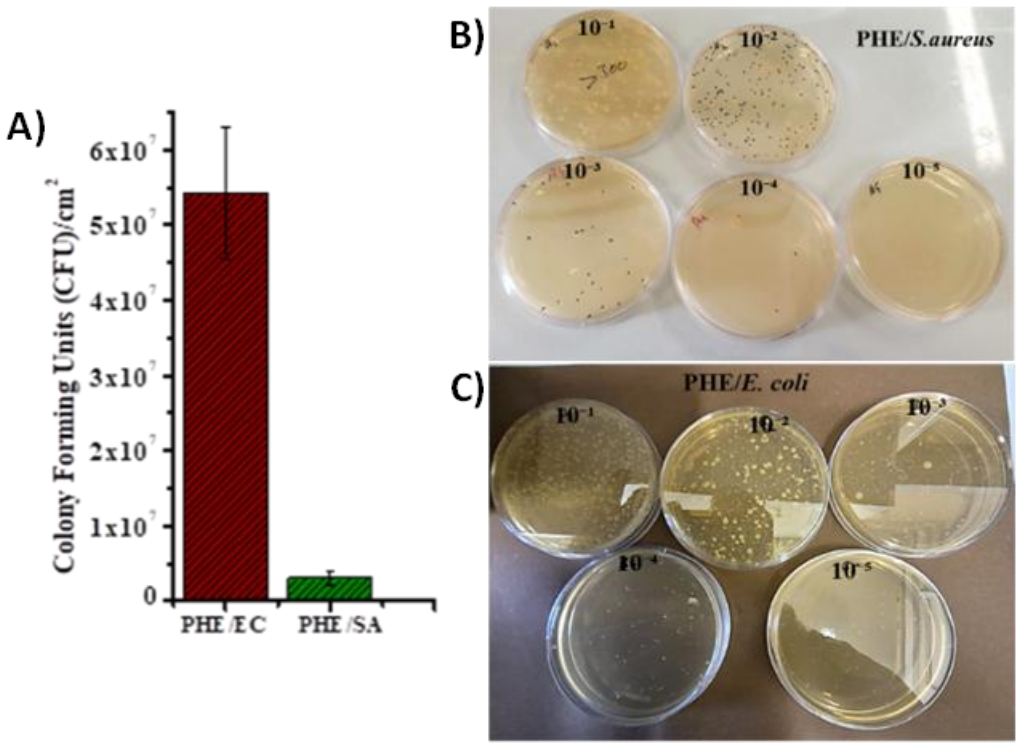

Figure S29. (A) Antibacterial effect of PHE-based polyHIPEs on the proliferation of *S. aureus (SA)* and *E. coli (EC),* with optical images of the petri dishes showing bacterial growth across serial dilutions: *S. aureus* **(B)** and *E. coli* **(C)**.